ChemComm

COMMUNICATION

View Article Online
View Journal | View Issue

Cite this: *Chem. Commun.*, 2017, 53, 5898

Received 10th April 2017,
Accepted 9th May 2017

DOI: 10.1039/c7cc02714a

rsc.li/chemcomm

High performance solution-processable tetrathienoacene (TTAR) based small molecules for organic field effect transistors (OFETs)†

Sureshraju Vegiraju,‡[a] Deng-Yi Huang,‡[b] Pragya Priyanka,[a] Yo-Shan Li,[a] Xian-Lun Luo,[b] Shao-Huan Hong,[b] Jen-Shyang Ni,[c] Shih-Huang Tung,[d] Chien-Lung Wang,[e] Wei-Chieh Lien,[a] Shueh Lin Yau,[a] Cheng-Liang Liu*[b] and Ming-Chou Chen*[a]

Three new organic semiconductors with alkyl chain-substituted tetrathienoacene (TTAR) as the central core and both ends capped with thiophene (DT-TTAR), thienothiophene (DTT-TTAR) and dithienothiophene (DDTT-TTAR) have been synthesized and characterized for organic field effect transistor (OFET) applications. A hole mobility of 0.81 $cm^2\ V^{-1}\ s^{-1}$ was achieved for the DDTT-TTAR film, which represents the highest mobility yet found for a solution-processable p-type TTAR-based small molecular semiconductors.

Solution-processable small molecular and polymeric semiconductors are of significant interest due to their potential low cost, mechanical flexibility, and compatibility compared to vacuum deposition semiconductors for OFETs.[1] With the advantages of structural versatility, facile synthesis, high purity, better reproducibility, and reliability without batch-to-batch variations, small molecules possess controllable electronic and physical properties compared to polymers.[2] Therefore, the development of small molecules for OFETs remains of particular interest. Among the well-known soluble small molecules, soluble pentacenes[3] and anthradithiophenes (ADT)[4] have been reported as promising materials that exhibit a carrier mobility as high as $>1\ cm^2\ V^{-1}\ s^{-1}$ in OFETs. However, low chemical stability in solution is a notable disadvantage of these soluble polyacenes, which normally suffer from oxidation in the presence of light and oxygen.[5] In the last decade, fused-thiophene based small molecules have emerged as alternative materials with excellent charge transport properties due to their unique features, such as extensive conjugation, strong intermolecular S–S interactions, and highly coplanar cores.[6] The fused-thiophene based units, such as thienothiophene (**TT**), dithienothiophene (**DTT**), tetrathienoacene (**TTA**), and pentathienoacene (**PTA**),[7] have not been fully explored for solution processed small molecules in OFETs and their device performance lagged behind those of benzannulated fused-acenes.[8] For example, **DP-DTT**,[2b] **PV-DTT**, **FPP-DTT**, **DDTT**,[9] **DP-TTA**,[7c] **PV-TTA**,[9a] and **PTA**[7d] (structures shown in Fig. S1 of ESI†) exhibit p-type mobilities in the range of 0.045 to 0.42 $cm^2\ V^{-1}\ s^{-1}$. In addition, **DFP-DTT**,[10] **DFP-TTA**,[6a] and **DFPT-TTA**[6b] exhibit n-type mobilities of up to 0.07, 0.30, and 0.43 $cm^2\ V^{-1}\ s^{-1}$, respectively. Due to their limited solubility, most of these materials have been fabricated by vacuum deposition techniques, and solution-processable small molecular organic semiconductors based on fused-thiophenes have barely been investigated to date. By substituting the alkyl side chains in the β-position of the fused-thiophene core, the solubility of the derived molecules could be achieved. Recently, our group developed a β-alkylated tetrathienoacene (**TTAR**)-based solution-processable small molecule **DDPP-TTAR** for OFETs, which exhibits a hole mobility of 0.1 $cm^2\ V^{-1}\ s^{-1}$.[11] Furthermore, the **TTAR**-based dye exhibits a power conversion efficiency of up to 10.1% in dye-sensitized solar cells, which could be attributed to the high transport characteristic of the **TTAR** core.[12] To further elaborate our study of this highly conjugated fused-thiophene core, in this work we explore **TTAR**-based solution-processable small molecules end-capped with thiophene (**DT-TTAR**; **1**), thienothiophene (**DTT-TTAR**; **2**), and dithienothiophene (**DDTT-TTAR**; **3**) for OFETs (see Scheme 1). A hole mobility of 0.81 $cm^2\ V^{-1}\ s^{-1}$ has been achieved for **DDTT-TTAR** *via* a solution-shearing process. To the best of our knowledge, currently this is the highest hole mobility for solution-processable **TTAR**-based small molecules.

The new **TTAR**s (**1–3**) were synthesized by the Stille coupling reaction of β-dialkylated dibromotetrathienothiophene (**4**) with stannylated thiophene (**5**), thienothiophene (**6**), and dithienothiophene (**7**), respectively. β-Dialkylated dibromotetrathienothiophene (**4**) and stannylated thiophenes (**5–7**) were prepared according to the

[a] *Department of Chemistry, National Central University, Taoyuan, 32001, Taiwan. E-mail: mcchen@ncu.edu.tw*
[b] *Department of Chemical and Materials Engineering, National Central University, Taoyuan, 32001, Taiwan. E-mail: clliu@ncu.edu.tw*
[c] *Institute of Chemistry, Academia Sinica, Taipei, 11529, Taiwan*
[d] *Institute of Polymer Science and Engineering, National Taiwan University, Taipei, 10617, Taiwan*
[e] *Department of Applied Chemistry, National Chiao Tung University, Hsinchu, 30010, Taiwan*

† Electronic supplementary information (ESI) available: Experimental details, synthesis, characterization, device fabrication and measurement, and theoretical calculation. See DOI: 10.1039/c7cc02714a

‡ These authors contributed equally.

Table 1 Thermal, optical and electrochemical properties of **DT-TTAR**, **DTT-TTAR** and **DDTT-TTAR**

Compound	T_d[a] (°C)	T_m[b] (°C)	λ_{abs} (solution) (nm)	λ_{abs} (film) (nm)	E_g[c] (eV)	E_{ox}[d] (V)	HOMO (eV)	LUMO (eV)
DT-TTAR (**1**)	386	120	390	374, 420	2.73	1.05	−5.25	−2.52
DTT-TTAR (**2**)	384	161	409	424, 457	2.44	1.01	−5.21	−2.77
DDTT-TTAR (**3**)	375	168	427	425, 469, 502	2.24	0.94	−5.14	−2.90

[a] Obtained from TGA. [b] Obtained from DSC. [c] Estimated from the onset of the absorption spectra. [d] Oxidative potential by DPV, Fc/Fc^+ was used as the internal standard and set at +0.6 V (−4.8 eV).

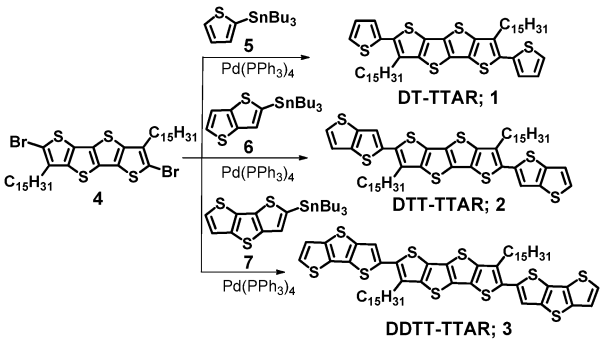

Scheme 1 Synthesis of **TTAR**s **1–3**.

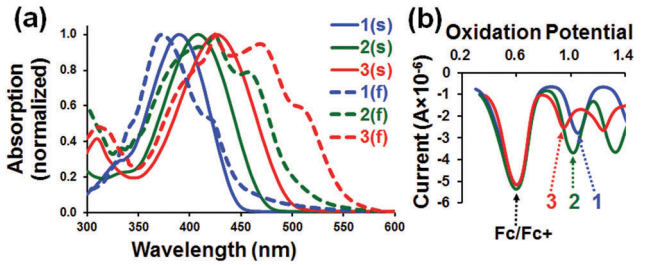

Fig. 1 (a) UV-Vis spectra of **1–3** in solution (denoted as S) and thin films (denoted as F). (b) DPV curves of **1–3** in 1,2-dichlorobenzene.

procedures in the literature.[13] These three newly synthesized **TTAR**s were purified by recrystallization, and exhibit adequate solubility in common organic solvents for solution processability in OFETs. The thermal behaviors of these three **TTAR**s were investigated by thermogravimetric analysis (TGA) and differential scanning calorimetry (DSC) under a nitrogen atmosphere, as shown in Fig. S2 of the ESI,† and are summarized in Table 1. All three new alkylated **TTAR**s underwent only ~5% weight loss when heated above 375 °C, indicating good thermal stability for their use in OFET applications. The DSC data revealed major endothermic melting peaks at 120, 161, and 168 °C for **DT-TTAR**, **DTT-TTAR**, and **DDTT-TTAR**, respectively. As expected, higher melting points are observed for **TTAR**s with higher molecular weights. Interestingly, **DTT-TTAR** exhibits another endothermic peak at 115 °C, which shows liquid crystal behavior of this compound.

UV-Vis spectra of these three **TTAR**s in dilute 1,2-dichlorobenzene solutions and thin films are shown in Fig. 1a, and the data are summarized in Table 1. With the increasing number of end-capped fused-thiophene units attached to the central **TTAR** core, the absorption maxima and the onset are significantly red-shifted from **DT-TTAR** to **DDTT-TTAR**. Greater π-electron delocalization is observed for the **DTT** end-capped derivative, giving the latter the lowest energy gap among the studied series. The absorption spectra of thin films of **DT-TTAR**, **DTT-TTAR**, and **DDTT-TTAR** are broadened relative to the solution spectra, mainly due to the intermolecular interactions within the films. As estimated from the onset of the thin film absorption, the optical energy gaps (E_g) of **DT-TTAR**, **DTT-TTAR**, and **DDTT-TTAR** are 2.73, 2.44, and 2.24 eV, respectively. This result indicates substantial delocalization extending from the end-capped thiophene substituents to the central **TTAR** core. The photooxidative stabilities of compounds **1–3** were investigated by monitoring the absorbance decay at λ_{max} in aerated 1,2-dichlorobenzene solutions while exposing them to white light (fluorescent lamp) at room temperature. Under ambient conditions (O_2 and H_2O present) no decomposition was observed over a month's period for these soluble compounds, demonstrating their potential as solution-processable organic semiconductors.

The electrochemical properties of these three **TTAR**-based compounds were analysed by differential pulse voltammetry (DPV). The oxidation peaks (E_{ox}) of **DT-TTAR**, **DTT-TTAR**, and **DDTT-TTAR** are exhibited at 1.05, 1.01, and 0.94 V, respectively, as shown in Fig. 1b. The derived HOMOs of **DT-TTAR**, **DTT-TTAR**, and **DDTT-TTAR** are thus estimated to be around −5.25, −5.21, and −5.14 eV, respectively, using the equation: HOMO = −(4.20 + E_{ox}) eV. As expected, the HOMO energy levels are upshifted from **DT-TTAR** to **DDTT-TTAR**, with the latter showing the most extensive π-electron delocalization. The LUMO energy levels were calculated from the correlation between the HOMO and the E_g, as summarized in Table 1. The electronic structure calculations were performed at the B3LYP/6-31G* level of density functional theory. The electronic profiles of the frontier molecular orbitals and the derived HOMO and LUMO values are shown in Fig. S3 of the ESI.† It was found that all the three **TTAR**s have similar electron density distributions on the HOMO and the LUMO, and the electron densities are delocalized on the whole conjugated framework. The extension of conjugation on the fused-thiophene capping moieties appears to lead to a further slight decrease in the LUMO and an upshift in the HOMO. The simulations also show that **DDTT-TTAR** has a smaller energy gap due to its extensive molecular conjugation, which is in good agreement with the electrochemical and optically derived data.

Solution-shearing crystalline OFETs were fabricated with three compounds onto a (2-phenylethyl)trichlorosilane (PETS)-modified Si/SiO_2 substrate.[14] Table 2 summarizes the field effect mobility (μ), threshold voltage (V_{th}), and the ON/OFF current ratio (I_{ON}/I_{OFF}) of the measured OFETs. The typical transfer and output curves for the OFETs are depicted in Fig. 2 and Fig. S4 (ESI†). In the case of **DT-TTAR**, the charge transport

Table 2 Summary of OFET parameters based on solution-sheared **DT-TTAR**, **DTT-TTAR**, and **DDTT-TTAR** thin films

Compound	μ_{max} [$cm^2\ V^{-1}\ s^{-1}$]	μ_{avg} [$cm^2\ V^{-1}\ s^{-1}$]	V_{th} [V]	I_{ON}/I_{OFF} [—]
DT-TTAR (1)	0.03	0.01 ± 0.01	−25 ± 6	10^4–10^5
DTT-TTAR (2)	0.12	0.07 ± 0.03	−15 ± 4	10^4–10^5
DDTT-TTAR (3)	0.81	0.31 ± 0.24	−10 ± 4	10^3–10^4

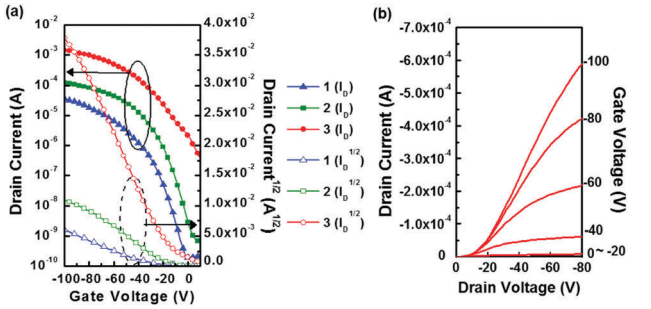

Fig. 2 (a) Transfer characteristics of OFETs for three solution-sheared films. (b) Output characteristics of **DDTT-TTAR** OFETs.

performance from the saturation region was optimized, with a maximum hole mobility (μ_{max}) and an average mobility (μ_{avg}) of up to 0.03 and 0.01 ± 0.01 $cm^2\ V^{-1}\ s^{-1}$, respectively, with a V_{th} of around −25 ± 6 V and an I_{ON}/I_{OFF} of 10^4–10^5. With an increase in the conjugation length of the capping groups, **DTT-TTAR** displays a much improved hole mobility at least four times higher compared to **DT-TTAR**. Notably, the crystalline **DDTT-TTAR** thin film shows the highest μ_{max} of 0.81 $cm^2\ V^{-1}\ s^{-1}$. These mobility data indicate that the increased molecular interaction of small molecular semiconductors upon increasing the conjugation length may contribute to the enhanced performance. The high OFF current observed for **DDTT-TTAR** may be because of the rough and thick crystalline semiconducting film,[15] resulting in a lower I_{ON}/I_{OFF} of 10^3–10^4. On the other hand, $|V_{th}|$ varies in the order of **DT-TTAR** > **DTT-TTAR** > **DDTT-TTAR**, which is mostly in agreement with the trends in the gap difference between the gold work function and HOMO energies. All thin film fabrication processes were conducted under ambient conditions, and the performance of **TTAR**-based p-type OFETs in different batches during ambient testing (relative humidity: 40–55%) did not degrade for at least 30 days (Fig. S5 of the ESI†).

Polarized optical microscopy (POM) and tapping mode atomic force microscopy (AFM) were utilized to investigate the crystalline morphology. The size of **DT-TTAR** crystallites is small, tens of micrometers, relative to the other two compounds (Fig. S6a, ESI†). As shown in Fig. S6b (ESI†), the **DTT-TTAR** film exhibits well-stacked elongated-shaped features growing along the shearing direction, while in Fig. S6c (ESI†), a blade-like crystal texture is seen in the **DDTT-TTAR** film and the slightly oriented crystallites may originate from the shearing force. It is found that the shearing process creates larger and more oriented grains, which along with the strong molecular interaction allows the **DDTT-TTAR** film to show a high charge transport ability. However, thin film morphologies strongly depend on the capping heterocyclic ring size of the **TTAR**-based

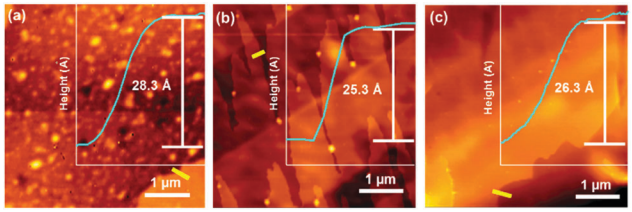

Fig. 3 AFM images and height profiles (along the yellow line) of solution-sheared (a) **DT-TTAR**, (b) **DTT-TTAR** and (c) **DDTT-TTAR** thin films.

compounds, as shown in the AFM image (Fig. 3a–c). **DT-TTAR** exhibits a multi-separated small crystalline plate-like structure with a plate height of ~28 Å (Fig. 3a). A large terrace-like crystalline microstructure in **DTT-TTAR** can be observed (Fig. 3b), which is the result of several continuous sublayers with a height of ~25 Å stacking in a layer-by-layer manner. In Fig. 3c, the high π–π interaction in **DDTT-TTAR** (as observed from the absorption spectrum) leads to a more integrated surface with much larger island-like crystallites (a height of ~26 Å). This continuous crystalline domain in **DDTT-TTAR** can possibly cross the channel gap between the source/drain electrodes, thus giving rise to the highest mobility found among all the three OFETs.

Grazing incidence X-ray diffraction (GIXRD) analysis was carried out, as shown in Fig. 4 and Fig. S7 of the ESI.† All the three compounds are highly crystalline and oriented with respect to the substrate, as determined from the patterns of multiple sharp diffraction spots. The peak positions of the out-of-plane scattering for the three films are at a 1:2:3 ratio, indicating a lamellar structure stacking normal to the films. The **DDTT-TTAR** film can even show the fourth-order peak. The *d*-spacing of the **DT-TTAR**, **DTT-TTAR**, and **DDTT-TTAR** thin films is 28.6, 25.4, and 27.0 Å, respectively, consistent with the layer thickness determined from the AFM height profiles (Fig. 3a–c). Fig. S8 of the ESI† shows the out-of-plane azimuthal scans on the (002) diffraction spots of the three samples. The width of the diffraction peaks along the azimuthal angle is the smallest for **DDTT-TTAR**, followed by **DTT-TTAR** and then **DT-TTAR**, implying that the orientation of the lamellae with respect to the substrate is in the order of **DDTT-TTAR** > **DTT-TTAR** > **DT-TTAR**. Through the correlations among the GIXRD

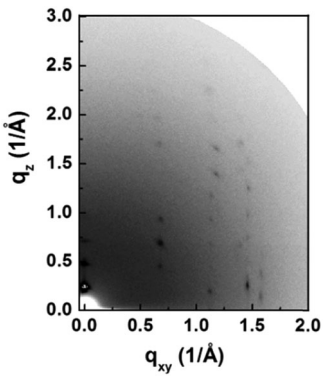

Fig. 4 GIXRD diffraction pattern image of a solution-sheared **DDTT-TTAR** thin film.

results, theoretical molecular lengths from the DFT calculations and AFM surface images, it can be concluded that all the three compounds are aligned on the substrate with an edge-on lamellar orientation, among which the **DDTT-TTAR** thin film shows the most regular stacking. **DTT-TTAR** and **DDTT-TTAR** exhibit more extensive intermolecular interactions,[16] and the molecular backbone is more preferentially aligned. The overall microstructural ordering and morphological features with large crystalline grains inside the organic semiconductor thin films are advantageous for efficient charge transport channels in OFETs.

In conclusion, three new β-alkylated **TTAR**-based small molecules with different capping π-conjugated molecules (**DT-TTAR**, **DTT-TTAR**, and **DDTT-TTAR**) were developed for solution-processable OFET applications. Importantly, it was found that compounds comprising longer conjugated capping groups derived from **DDTT-TTAR** produce stronger molecular interactions, contributing to the morphological formation of large crystalline grains and a better molecular packing distribution in the azimuth. The OFETs based on solution-sheared **DT-TTAR**, **DTT-TTAR**, and **DDTT-TTAR** thin films showed hole mobilities of up to 0.03, 0.12, and 0.81 $cm^2 V^{-1} s^{-1}$, respectively, with an I_{ON}/I_{OFF} of 10^3–10^5, making **DDTT-TTAR** the highest solution-processable hole transporting **TTAR**-based small molecule reported to date. Complementary thin film surface microstructures and morphologies were characterized by POM, AFM and GIXRD to correlate with the performance of OFETs. The findings reported here will be important for enabling the molecular design of novel solution-processable organic semiconductors for OFET applications.

This work was supported by the Ministry of Science and Technology (MOST) of Taiwan. The authors thank Beamline B13A1/B17A1 (National Synchrotron Radiation Research Center (NSRRC) of Taiwan) for providing beamtime.

Notes and references

1 S. Allard, M. Forster, B. Souharce, H. Thiem and U. Scherf, *Angew. Chem., Int. Ed.*, 2008, **47**, 4070–4098.
2 (*a*) W. Jiang, Y. Li and Z. Wang, *Chem. Soc. Rev.*, 2013, **42**, 6113–6127; (*b*) Y. M. Sun, Y. Q. Ma, Y. Q. Liu, Y. Y. Lin, Z. Y. Wang, Y. Wang, C. A. Di, K. Xiao, X. M. Chen, W. F. Qiu, B. Zhang, G. Yu, W. P. Hu and D. B. Zhu, *Adv. Funct. Mater.*, 2006, **16**, 426–432.
3 (*a*) T.-H. Chao, M.-J. Chang, M. Watanabe, M.-H. Luo, Y. J. Chang, T.-C. Fang, K.-Y. Chen and T. J. Chow, *Chem. Commun.*, 2012, **48**, 6148–6150; (*b*) J. E. Anthony, J. S. Brooks, D. L. Eaton and S. R. Parkin, *J. Am. Chem. Soc.*, 2001, **123**, 9482–9483.
4 (*a*) M. M. Payne, S. R. Parkin, J. E. Anthony, C.-C. Kuo and T. N. Jackson, *J. Am. Chem. Soc.*, 2005, **127**, 4986–4987; (*b*) M.-C. Chen, C. Kim, S.-Y. Chen, Y.-J. Chiang, M.-C. Chung, A. Facchetti and T. J. Marks, *J. Mater. Chem.*, 2008, **18**, 1029–1036.
5 (*a*) H.-C. Yu, G. Kwon, S. Vegiraju, C.-W. Chao, L.-H. Li, J.-S. Ni, P.-Y. Huang, S. L. Yau, Y.-C. Chao, C. Kim and M.-C. Chen, *Dyes Pigm.*, 2016, **126**, 261–269; (*b*) C. Kim, P.-Y. Huang, J.-W. Jhuang, M.-C. Chen, J.-C. Ho, T.-S. Hu, J.-Y. Yan, L.-H. Chen, G.-H. Lee, A. Facchetti and T. J. Marks, *Org. Electron.*, 2010, **11**, 1363–1375.
6 (*a*) J. Youn, P.-Y. Huang, Y.-W. Huang, M.-C. Chen, Y.-J. Lin, H. Huang, R. P. Ortiz, C. Stern, M.-C. Chung, C.-Y. Feng, L.-H. Chen, A. Facchetti and T. J. Marks, *Adv. Funct. Mater.*, 2012, **22**, 48–60; (*b*) J. Youn, S. Vegiraju, J. D. Emery, B. J. Leever, S. Kewalramani, S. J. Lou, S. Zhang, K. Prabakaran, Y. Ezhumalai, C. Kim, P.-Y. Huang, C. Stern, W.-C. Chang, M. J. Bedzyk, L. X. Chen, M.-C. Chen, A. Facchetti and T. J. Marks, *Adv. Electron. Mater.*, 2015, **1**, 1500098.
7 (*a*) Q. Wu, S. Ren, M. Wang, X. Qiao, H. Li, X. Gao, X. Yang and D. Zhu, *Adv. Funct. Mater.*, 2013, **23**, 2277–2284; (*b*) M.-C. Chen, Y.-J. Chiang, C. Kim, Y.-J. Guo, S.-Y. Chen, Y.-J. Liang, Y.-W. Huang, T.-S. Hu, G.-H. Lee, A. Facchetti and T. J. Marks, *Chem. Commun.*, 2009, 1846–1848; (*c*) Y. Liu, Y. Wang, W. Wu, Y. Liu, H. Xi, L. Wang, W. Qiu, K. Lu, C. Du and G. Yu, *Adv. Funct. Mater.*, 2009, **19**, 772–778; (*d*) K. Xiao, Y. Liu, T. Qi, W. Zhang, F. Wang, J. Gao, W. Qiu, Y. Ma, G. Cui, S. Chen, X. Zhan, G. Yu, J. Qin, W. Hu and D. Zhu, *J. Am. Chem. Soc.*, 2005, **127**, 13281–13286.
8 (*a*) Y. Yuan, G. Giri, A. L. Ayzner, A. P. Zoombelt, S. C. B. Mannsfeld, J. Chen, D. Nordlund, M. F. Toney, J. Huang and Z. Bao, *Nat. Commun.*, 2014, **5**, 3005; (*b*) T. Mori, T. Nishimura, T. Yamamoto, I. Doi, E. Miyazaki, I. Osaka and K. Takimiya, *J. Am. Chem. Soc.*, 2013, **135**, 13900–13913.
9 (*a*) Y. Liu, C.-A. Di, C. Du, Y. Liu, K. Lu, W. Qiu and G. Yu, *Chem. – Eur. J.*, 2010, **16**, 2231–2239; (*b*) M.-C. Chen, S. Vegiraju, C.-M. Huang, P.-Y. Huang, K. Prabakaran, S. L. Yau, W.-C. Chen, W.-T. Peng, I. Chao, C. Kim and Y.-T. Tao, *J. Mater. Chem. C*, 2014, **2**, 8892–8902; (*c*) X.-C. Li, H. Sirringhaus, F. Garnier, A. B. Holmes, S. C. Moratti, N. Feeder, W. Clegg, S. J. Teat and R. H. Friend, *J. Am. Chem. Soc.*, 1998, **120**, 2206–2207.
10 C. Kim, M.-C. Chen, Y.-J. Chiang, Y.-J. Guo, J. Youn, H. Huang, Y.-J. Liang, Y.-J. Lin, Y.-W. Huang, T.-S. Hu, G.-H. Lee, A. Facchetti and T. J. Marks, *Org. Electron.*, 2010, **11**, 801–813.
11 N. Zhou, S. Vegiraju, X. Yu, E. F. Manley, M. R. Butler, M. J. Leonardi, P. Guo, W. Zhao, Y. Hu, K. Prabakaran, R. P. H. Chang, M. A. Ratner, L. X. Chen, A. Facchetti, M.-C. Chen and T. J. Marks, *J. Mater. Chem. C*, 2015, **3**, 8932–8941.
12 (*a*) N. Zhou, K. Prabakaran, B. Lee, S. H. Chang, B. Harutyunyan, P. Guo, M. R. Butler, A. Timalsina, M. J. Bedzyk, M. A. Ratner, S. Vegiraju, S. Yau, C.-G. Wu, R. P. H. Chang, A. Facchetti, M.-C. Chen and T. J. Marks, *J. Am. Chem. Soc.*, 2015, **137**, 4414–4423; (*b*) Y. Ezhumalai, B. Lee, M.-S. Fan, B. Harutyunyan, K. Prabakaran, C.-P. Lee, S. H. Chang, J.-S. Ni, S. Vegiraju, P. Priyanka, Y.-W. Wu, C.-W. Liu, S. Yau, J. T. Lin, C.-G. Wu, M. J. Bedzyk, R. P. H. Chang, M.-C. Chen, K.-C. Ho and T. J. Marks, *J. Mater. Chem. A*, 2017, **5**, DOI: 10.1039/c7ta01825h.
13 S. Vegiraju, Y.-Y. Liu, K. Prabakaran, J.-S. Ni, Y. Ezhumalai, H.-C. Yu, S. L. Yau, J. T. Lin, M.-C. Chen and T.-C. Lin, *RSC Adv.*, 2015, **5**, 54003–54010.
14 (*a*) Y. Diao, B. C. K. Tee, G. Giri, J. Xu, D. H. Kim, H. A. Becerril, R. M. Stoltenberg, T. H. Lee, G. Xue, S. C. B. Mannsfeld and Z. Bao, *Nat. Mater.*, 2013, **12**, 665–671; (*b*) G. Giri, E. Verploegen, S. C. B. Mannsfeld, S. Atahan-Evrenk, D. H. Kim, S. Y. Lee, H. A. Becerril, A. Aspuru-Guzik, M. F. Toney and Z. Bao, *Nature*, 2011, **480**, 504–508.
15 K. Fukuda, Y. Takeda, M. Mizukami, D. Kumaki and S. Tokito, *Sci. Rep.*, 2014, **4**, 3947.
16 T. K. An, S. H. Jang, S.-O. Kim, J. Jang, J. Hwang, H. Cha, Y. R. Noh, S. B. Yoon, Y. J. Yoon, L. H. Kim, D. S. Chung, S.-K. Kwon, Y.-H. Kim, S.-G. Lee and C. E. Park, *Chem. – Eur. J.*, 2013, **19**, 14052–14060.